Roles of nitrogen substitution and surface reconstruction in stabilizing nonpassivated single-layer diamond

T. Pakornchote,[1,2] A. Ektarawong,[1,2] W. Busayaporn,[3] U. Pinsook,[1,2] and T. Bovornratanaraks[1,2,*]

[1]*Extreme Condition Physics Research Laboratory, Physics of Energy Materials Research Unit, Department of Physics, Faculty of Science, Chulalongkorn University, Bangkok 10330, Thailand*

[2]*Thailand Center of Excellence in Physics, Commission on Higher Education, 328 Si Ayutthaya Road, Bangkok 10400, Thailand*

[3]*Synchrotron Light Research Institute (Public Organization), Nakhon Ratchasima, 30000, Thailand*

(Received 12 April 2020; revised 20 July 2020; accepted 21 July 2020; published 10 August 2020)

The existence of single-layer diamond or diamane, which could adopt the properties of its bulk counterpart, has been verified by previous calculations and experiments. Even though, carbon atoms on the top and bottom surfaces need to form dangling bonds with atoms and/or molecules to stabilize their sp^3 hybridization. In this paper, diamane is substituted by N atoms assisting the diamondlike structure to be stabilize without any passivation studied by *ab initio* calculation. One-fourth of N substitution on diamane, vertically stacking as NCCC, is found to be stable by surface reconstruction forming a Pandey π-chain structure and has an antiferromagnetic property. Half nitrogen substitution on diamane, vertically stacking as NCCN, can be stable and prevails the diamane form. Its elastic constants yield high values, for example, its C_{11} is as twice as diamond and its C_{33} is only 21% lower than diamond. The NCCN phase is a metastable phase at 10 GPa compared with other layered carbon nitride phases showing the possible pathway to be created.

DOI: 10.1103/PhysRevB.102.075418

I. INTRODUCTION

A single-layer diamond or diamane is prospected to be the thinnest hardness material. It can be created by tipping on bilayer graphene (BLG) to create the sp^3 bonding between interlayer carbon atoms enhancing the hardness of its substrate [1,2]. A layer of sp^3 carbon, however, cannot sustain its structure without the tipping force [1]. The well-known problem is, for example, a surface reconstruction of bulk diamond. The surface of bulk diamond is either buckling, reconstructing the surficial layer or terminated by atoms and/or molecules in order to lower the potential-energy surface [3–8]. For diamane, the carbon atoms at the top and bottom layers have to be passivated by atoms and/or molecules, e.g., H, OH, and F, in order to stabilize diamane making the passivated diamane metastable [9–13]. Diamane, whose dangling bonds on the surface are passivated by OH molecules, could be created at 5 GPa [13] the same as diamond which typically becomes a stable phase at high pressure.

Martins *et al.* [13] used multiwavelength Raman spectroscopy to show that the *G* peak of BLG is discrepant in frequency between two wavelength lasers at 5 GPa. The results state that the dangling bonds of C atoms form sp^3 hybridization by passivating with OH, however, this transition occurs in the partial area of the sample whereas the other areas were still sp^2 hybridization. The sp^3 carbon did not sustain when the sample was retrieved to ambient pressure. The passivated diamane can also be synthesized at low pressure by hot filament and chemical vapor deposition (CVD) techniques [14,15]. The stability is better if the passivation is on both sides of diamane whereas one-side passivation is also possible for few-layer graphene [16]. The fluorinated diamane has been successfully synthesized by treating fluorine onto BLG for 12 h. The time is sufficient for F atoms penetrating through BLG, so the fluorinated diamane can be formed by two-side passivation as shown by the image from a scanning electron microscope [15].

In the present paper, a N atom, which has one valence electron more than a C atom, is considered to substitute in diamane instead of the passivation. In our hypothesis, an extra electron could form an electron lone pair which decreases the potential-energy surface the same as the passivation. Hence, a N atom, whose atomic radius is similar to a C atom, is the choice of study. Rather than hydrogenation or fluorination, N substitution in diamane is a two-dimensional (2D) carbon nitride which could adopt the superhard property, such as in bulk carbon nitrides. Diamane is a diamond thinned down in the [111] direction until it has four C atoms in a unit cell by vertically stacking as CCCC leaving two lone electrons on the surface. The substitution of the N atom on a surficial C atom automatically creates the lone electron pair and could stabilize the diamanelike structure. Four configurations of N-substituted diamane ($C_{4-x}N_x$), derived from the unit cell of diamane with $x = 1$ and 2 by vertically stacking as NCCC, CNCC, NCCN, and CNCN, are herein considered. Some of their intrinsic properties, i.e., elastic constants, electronic band structures, and density of states (DOS), magnetism and phase transitions will be investigated and discussed.

II. COMPUTATIONAL METHOD

The density functional theory implemented in the Vienna *ab initio* simulation package (VASP) was employed using

*thiti.b@chula.ac.th

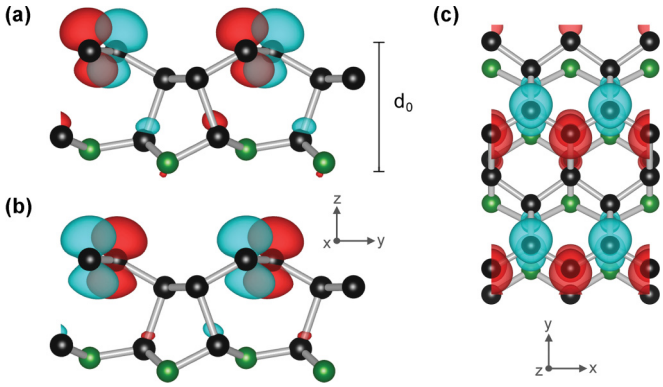

FIG. 1. The relaxed structure of π-C_3N in (a) the [100] direction and (d) the [001] direction where the blue and red envelopes are positive and negative magnetization densities, respectively, of the valence-band maximum at the K point and (b) of the conduction-band minimum at the J point. Black and green balls represent C and N atoms, respectively.

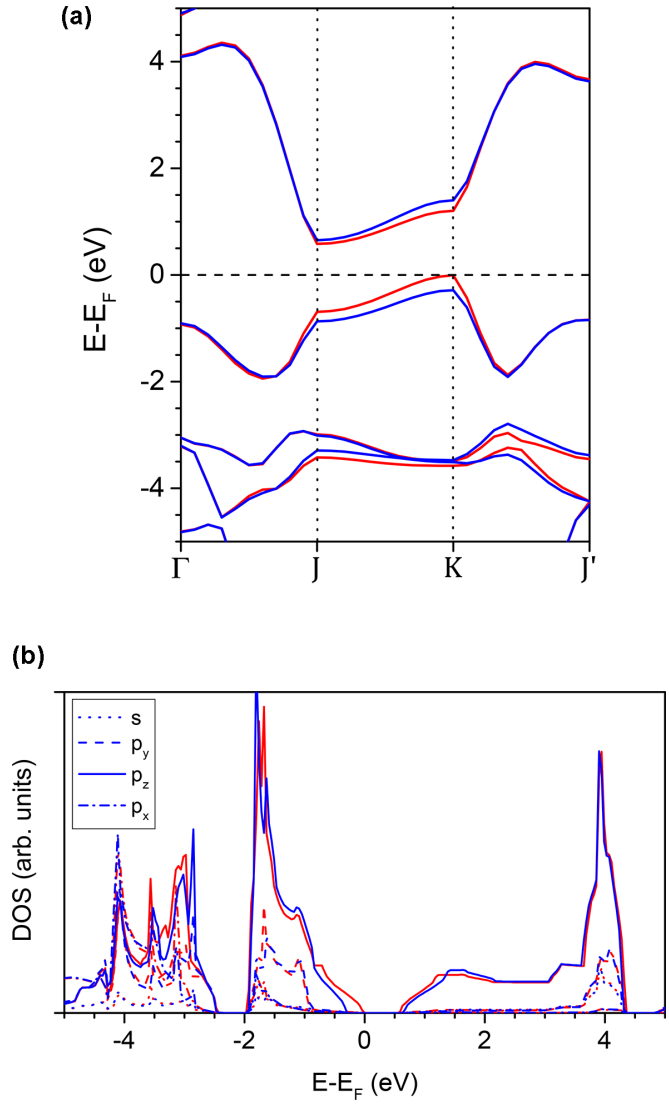

FIG. 2. (a) Band dispersion shows the splitting between spin-up (blue) and spin-down (red) bands. (b) The partial electronic DOS of π-C_3N is projected onto s (dotted), p_y (dashed), p_z (line), and p_x (dashed dotted) of a C atom where blue and red present spin-up and spin-down DOS, respectively.

the projector augmented-wave method for the pseudopotential [17–20]. The Perdew-Burke-Ernzerhof (PBE) exchange-correlation functional was used for relaxing crystal structures, and the Heyd-Scuseria-Ernzerhof (HSE06) screen exchange hybrid functional was used for calculating the energy gap by using the relaxed structures from PBE [21,22]. In order to ensure the convergence of the energy, the cutoff energy was set as 600 eV, and the k points were meshed using the Monkhorst-Pack scheme [23,24]. The van der Waals correction using the DFT-D3 method of Grimme *et al.* was included for all calculations presented in this paper [25]. To solve for phonon and vibrational schemes using the finite displacement method implemented in the PHONOPY package [26,27], VASP was used to calculate forces on each atomic in a deviated crystal with $5 \times 5 \times 1$ and $3 \times 3 \times 3$ supercells for single-layer and bulk systems, respectively. The previous study shows that the magnetism of the diamond surface is absent when using PBE but present when using PBE0 and HSE06 [28]. Therefore, in this paper, the collinear spin-polarized method together with HSE06 were employed to study the magnetic property of N-substituted diamane.

III. RESULTS AND DISCUSSION

A. Structure, magnetism, and electronic properties

Certainly, diamane, which has four C atoms vertically stacking as CCCC, transforms to BLG after structural relaxation [12]. Two of diamane substituted by one N atom (C_3N) vertically stacking as NCCC and CNCC also transform to a layer of graphene and CN after structural relaxation. Therefore, for NCCC, one side of the N substitution forming one-side electron lone pairs is not sufficient for the energy of the system to be the local minimum and stabilize the sp^3 bonding between layers. A graphene side is then reconstructed to be the Pandey π chain using a rectangular cell (see Fig. 1) in order to lower the potential-energy surface from lone electrons on the surface [4]. In contrast to the diamane form, the reconstructed NCCC (π-C_3N) does not transform back to a layer of graphene and CN after structure relaxation as depicted in Fig. 1 (see Table S1 in the Supplemental Material [29] for structure parameters). It is also dynamically stable verified by a phonon calculated using the PBE functional where the vibrational frequencies are listed in Table S2 of the Supplemental Material [29]. It is worth noting that the one-side Pandey π chain forms of CCCC and CNCC are not stable by separating to two layers after structural relaxation.

The magnetic property of π-C_3N is investigated using a collinear spin-polarized calculation with PBE and HSE06 functionals resulting in the absence and presence of magnetism in π-C_3N, respectively, in agreement with Ref. [28]. The antiferromagnetic (ferromagnetic) phase of π-C_3N has an energy 5.8 meV per unit cell lower (2.9 eV per unit cell higher) than its nonmagnetic phase, so the antiferromagnetic phase is energetically favorable. Moreover, π-C_3N is antiferromagnetic with zero total magnetization in contrast to the diamond surface which is ferrimagnetic. The magnetization

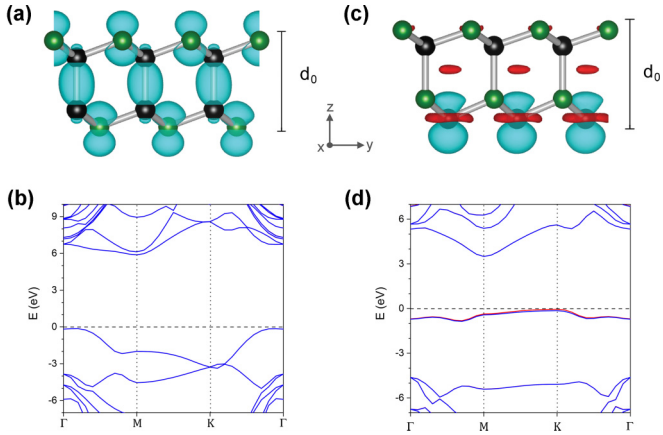

FIG. 3. (a) The relaxed structure of NCCN is presented by projecting in the [100] direction where blue envelopes are the spin-up charge density of valence-band maximum at the Γ point. The relaxed structure of CNCN is presented by projecting in the [100] direction where blue and red envelopes are positive and negative magnetization densities, respectively, of the valence-band maximum at the K point. (b) and (d) are band structures of NCCN and CNCN, respectively. Black and green balls represent C and N atoms, respectively.

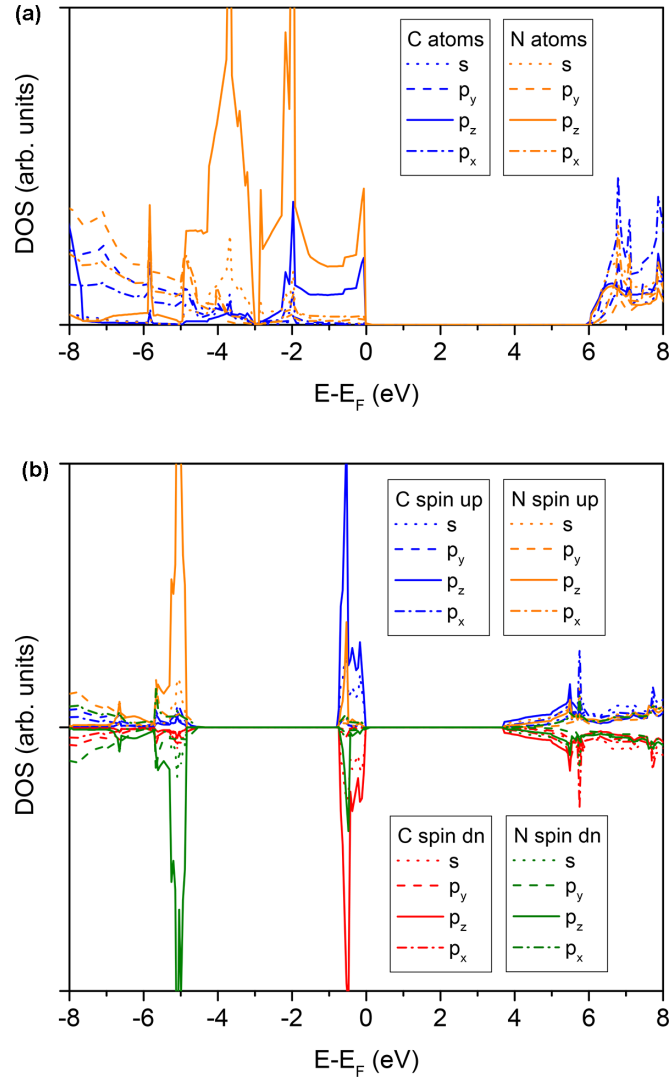

FIG. 4. Electronic partial DOS of (a) NCCN and (b) CNCN are presented in color for the spin up of the C atom (blue) and the N atom (orange) and the spin down of the C atom (red) and N atom (green). The projected orbitals are presented in dotted, dashed, solid, and dashed-dotted lines for s, p_y, p_z, and p_x orbitals, respectively. Note that spin-up and spin-down DOS of NCCN are identical, so only spin-up DOS is shown.

is mostly from the top two C atoms obtaining $0.130\mu_B$ and $-0.128\mu_B$. The valence-band maximums of spin up and spin down largely split along the J-to-K path [see Fig. 2(a)]. The energy gaps from spin up and spin down are indirect from a ground state at the K point to an excited state at the J point with 0.93 and 0.59 eV, respectively. The valance states on the J-to-K path are from the p_z orbital depicted as a partial charge density adopting a shape of the π-bonding envelope [see Figs. 1 and 2(b)]. The envelopes of spin-up and spin-down charge densities are residing at the top C atoms resulting in the direction of magnetization alternating along the x axis resembling a chain [see Fig. 1(c)]. The partial charge density of the conduction-band minimum at the J point shows a feature of π antibonding where the charge densities of spin up and spin down are at C atoms alternating with that of the valence-band maximum at the K point.

For C_2N_2, two configurations of N-substituted diamane vertically stacking as NCCN and CNCN are studied [see Figs. 3(a) and 3(c)]. NCCN and CNCN are energetically stable after structural relaxation. However, only NCCN is dynamically stable (see Fig. S2 in Supplemental Material [29]). Moreover, collinear spin-polarized calculation with the HSE06 functional is employed in order to determine the magnetism of NCCN and CNCN. In contrast to π-C_3N, the magnetism of NCCN is absent, and CNCN has a tiny magnetization of $0.007\mu_B$. For CNCN, the magnetism mainly arises from C atoms. The surficial C atoms and inner C atoms have magnetizations about $0.008\mu_B$ and $-0.001\mu_B$, respectively.

For NCCN, the electronic band dispersion shows no splitting between spin up and spin down as a result in the absence of magnetism [see Fig. 3(b)]. The valence states are mainly from the p_z orbital of C and N atoms as depicted in Fig. 4(a). For CNCN, its valence-band maximum is nearly flat causing high density of states near the Fermi level and only this band that has a splitting between spin up and spin down [see Fig. 3(d)]. The valence states are mainly from s and p_z orbitals of the C atom on the surface as depicted in Fig. 4(b). The remark feature is in-between -4 and -6 eV below the Fermi level where the p_z orbital of the N atom on the surface becomes a main contribution. It can be indicated that the N atom on the surface contributes energy to the system lower than if the C atom is on the surface so that results in reducing the potential-energy surface. The energy gaps derived from HSE06 are 6.1 and 4.4 eV for NCCN and CNCN, respectively.

For CNCN, its bulk counterpart is dynamically stable [30], hence, the single-layer phase could be dynamically stabilized if the carbon side sits on a substrate. This phase exhibiting ferromagnetic behavior could be used as a 2D magnetic semiconductor [31] with a high concentration of holes since it has a surprisingly large density of states at the Fermi level [32].

TABLE I. The 2D elastic constants of single-layer NCCN, CNCN, π-C_3N, H-diamane, graphene, and SiC in N/m units.

Phase	C_{11}^{2D}	C_{12}^{2D}	C_{13}^{2D}	C_{22}^{2D}	C_{33}^{2D}	C_{44}^{2D}	C_{66}^{2D}
NCCN	568	66	51		217	66	243
CNCN	526	61	38		170		220
π-C_3N	595	106	27	510	159		244
H-diamane[a]	487	38					
Graphene[b]	358	60					
SiC[c]	179	57					

[a]Reference [12].
[b]Reference [34].
[c]Reference [35].

B. Elastic constants

Some phases of carbon nitride were predicted to be superhard materials by which its cubic phase is even harder than diamond [33]. A bulk NCCN was shown that it has high elastic constant C_{11}, however, it came with low C_{33} [30]. In a perspective of 2D materials, BLG can resist the indented force better than graphite which is its bulk counterpart [1]. Since the volume of 2D materials, e.g., single-layer graphene, is not well defined, 2D elastic constant (C_{ij}^{2D}), which has a N/m unit [34,35], evaluated with respect to pure C and N phases, and can be expressed as

$$C_{ij}^{2D} = \frac{1}{A_0}\left(\frac{\partial^2 E(\varepsilon_1, \ldots, \varepsilon_6)}{\partial\varepsilon_i \partial\varepsilon_j}\right), \quad (1)$$

where A_0 is the unstrained in-plane area of layered C_xN_y and ε_i is the applied strain up to $\pm 2\%$ of the lattice parameters where $i = 1, \ldots, 6$ and 1–6 are xx, yy, zz, yz, zx, and xy, respectively, in Cartesian coordinates. The x-y plane is an in-plane direction, and z is an out-of-plane direction where in the present paper, 11 and 22 are along the zigzag and armchair directions, respectively. In fact, the N-substituted diamanes are not 1-at. thick, but it has a semithird dimension by which the sp^3 bonding is on the z axis. Their elastic constants (C_{ij}) could be calculated by dividing with the effective height (d_0) which is a vertical distance between top and bottom atoms perpendicularly to the in-plane section,

$$C_{ij} = \frac{1}{d_0 A_0}\left(\frac{\partial^2 E(\varepsilon_1, \ldots, \varepsilon_6)}{\partial\varepsilon_i \partial\varepsilon_j}\right), \quad (2)$$

where $d_0 = 2.93$, 2.59, and 2.67 Å for π-C_3N, NCCN, and CNCN, respectively. Because the N-substituted diamanes have the effective thickness, so C_{ij} in the out-of-plane direction, i.e., C_{13}, C_{33}, and C_{44} are herein reported. The calculations by leaving the z direction unconstrained will give a bad result, then, one may see the Supplemental Material [29] for the calculation procedure in VASP to obtain a reasonable result.

Table I presents the comparison of C_{ij}^{2D} between several 2D materials. Obviously, single layers of NCCN, CNCN, π-C_3N, and hydrogenated diamane (H-diamane) have C_{ij}^{2D} higher than single layers of graphene and SiC [12,34,35]. Therefore, the diamondlike structure yields C_{ij}^{2D} higher than the flat structure, e.g., single-layer graphene. The reason is that C_{ij}^{2D} is an intrinsic property for the flat structure since it lacks a third dimension, however, C_{ij}^{2D} is an extrinsic property for the diamondlike structure. The energy used to stretch 2D materials is higher with thickness. Thus, those C_{ij}^{2D}'s have to be divided by the thickness yielding C_{ij}.

TABLE II. The bulk elastic constants of single-layer phases which are NCCN, CNCN, π-C_3N, and H-diamane, and their bulk counterparts in GPa units.

	Phase	C_{11}	C_{12}	C_{13}	C_{22}	C_{33}	C_{44}	C_{66}
Single-layer	NCCN	2191	253	198		836	256	939
	CNCN	1968	227	142		635		825
	π-C_3N	2030	361	91	1739	541		831
	H-diamane[a]	1026	81					
Bulk	NCCN[b]	965	107	−10		59	10	430
	CNCN[b]	929	102	3		73	37	414
	Diamond[a]	1051	127					559
	Diamond[c]	1079	124				578	

[a]Reference [12]—DFT.
[b]Reference [30]—DFT.
[c]Reference [37]—experiment.

Since the N-substituted diamanes have thicknesses from the semithird dimension, C_{ij}'s were evaluated in order to compare with bulk materials. Table II lists the C_{ij} of two phases of C_2N_2 in comparison with the bulk diamond. C_{11}, C_{66}, and C_{12} of NCCN yield about two times higher than diamond and H-diamane whereas its C_{33} is about 20% lower than diamond, and its C_{44} is about half of that of diamond. CNCN yields a similar result to NCCN. Therefore, NCCN and CNCN are tougher (softer) than diamond in the in-plane (out-of-plane) direction and more vulnerable to shearing indicated by the comparison of C_{44}. We want to state that Eq. (2) could be just the upper limit of C_{ij} where the lower limit is when d_0 is the height of the bulk form reported in Ref. [30]. The Born stability criteria [36] was considered and found that both NCCN and CNCN are mechanically stable. For π-C_3N, its C_{11} is as much as C_{11} of NCCN, its C_{22} is a bit smaller than C_{22} of NCCN, and its C_{33} is significantly lower than with C_{33} of NCCN. It is worth marking that C_{22}, a response in an armchair direction, is lower than C_{11}, a response in a zigzag direction.

The elastic constants of N-substituted diamanes in the present paper are as high as bulk superhard materials. Thus, they potentially are superhard coating materials as demonstated that BLG can enhance a resistance to the indentation of its substrate [1]. Nevertheless, to the best of our knowledge, the hardness of 2D materials is inconclusive and needs more explorations.

C. Synthesizability

To pursue the possibility of further syntheses of NCCN, CNCN, and π-C_3N, the formation enthalpy (ΔH_{form}) of carbon nitride systems was evaluated by

$$\Delta H_{\text{form}}(C_xN_y) = H(C_xN_y) - \frac{xH(C) + yH(N)}{x + y}, \quad (3)$$

where x and y, respectively, are the numbers of C and N atoms in the system, and the enthalpy terms on the right-hand side are the enthalpies of those systems per atom. The pure C and N phases used as reference phases at 0 GPa are BLG

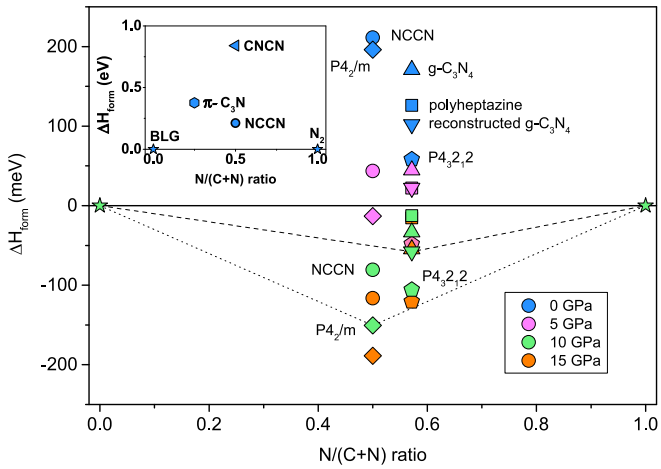

FIG. 5. The formation enthalpy of carbon nitrides at 0, 5, 10, and 15 GPa is plotted with respect to pure C and N phases (star symbol). The carbon nitride phases included in the diagram are NCCN (circle), CNCN (left triangle), π-C_3N (hexagon), g-C_3N_4 (triangle), polyheptazine (square), reconstructed g-C_3N_4 (down triangle), $P4_2/m$ (diamond), and $P4_32_12$ (pentagon). The dashed (dotted) line is a convex hull connecting between diamond and reconstructed g-C_3N_4 ($P4_2/m$-CN) and $P4_12_12$-N_2.

and N_2, respectively. Some stable phases of carbon nitride are included in the phase diagram where they can be considered as two types; layered and nonlayered morphologies. The layered phases of carbon nitride are g-C_3N_4, reconstructed g-C_3N_4, and polyheptazine [38,39] (the structures are provided in Table S5 in the Supplemental Material [29]) that could be a starting material of N-substituted diamanes. For the nonlayered phases, the structures included in the phase diagram are $P4_32_12$-C_3N_4 and $P4_2/m$-CN, which are energetically favorable phases among their stoichiometries at pressures considered in the phase diagram [39,40].

The inset in Fig. 5 shows that ΔH_{form} at 0 GPa of NCCN, CNCN, and π-C_3N are 211, 839, and 375 meV, respectively. Since their ΔH_{form}'s are even higher than other carbon nitrides (see Fig. 5), these phases cannot be formed by using BLG or other carbon nitrides as precursors at ambient pressure. Likewise, diamond has enthalpy lower than graphite at 5 GPa, the study, hence, has been further investigated at high pressure. The reference phases, changed from BLG and the N_2 molecule, are diamond for the pure C phase at 5–20 GPa, and for the pure N phase, the $P2_1/c$ phase at 5 GPa, and the $P4_12_12$ phase at 10–20 GPa [41]. At ambient pressure, the N-substituted diamanes are considered as single layers, however, at high pressure, the compression in the out-of-plane direction is inevitable and must be taken into account in the calculation. The c axis is allowed to be relaxed in order to create isotropic pressure around materials trading-off with that NCCN and others are no longer the single-layer phases.

Figure 5 shows the phase diagram of carbon nitrides comparing with C phases and N phases at ambient and under high pressure. CNCN and π-C_3N have a ΔH_{form} higher than NCCN even at high pressure, so only NCCN will be herein discussed. As depicted in Fig. 5, the ΔH_{form} of NCCN decreases steeply from 211 meV at ambient pressure to 43.5 meV at 5 GPa and −83.3 meV at 10 GPa. The dashed lines are illustrated as a convex hull connecting with reconstructed g-C_3N_4 and showing that the ΔH_{form} of NCCN is the lowest among layered phases at 10 GPa. Although, it is higher than nonlayered phases, i.e., $P4_2/m$ and $P4_32_12$ as illustrated as a dotted convex hull. In the graphene case, it can be recovered from high pressure without buckling [13,42,43], hence, it is possible to synthesize the N-substituted diamane from bilayer carbon nitrides without transforming to nonlayered phases. However, in order to synthesize the N-substituted diamane using a high-pressure pathway, the stacking of the bilayer and pressure medium are crucial and must be designedly chosen. For example, AB-stacking BLG is more beneficial for synthesizing fluorinated diamane than AA stacking and twisted BLGs [15].

Typically, diamond is a stable phase at 5 GPa, but it can be synthesized at hundreds of millibars using the CVD technique. N substitution in diamond is created by feeding the N compound, e.g., N_2, and $(NH_2)_2CO$ as a dopant during the growth process [44,45]. One interpretation of the present paper indicates that the N-terminated diamond surface could be stable if the surface is merely filled by N atoms. One would expect that NCCN might be achieved using the CVD technique, however, the real experiment is challenging, and further theoretical investigation to serve the experiment is needed.

IV. CONCLUSIONS

In conclusion, we present the stabilization of the N substitution in diamane. The substitution of one N atom in diamane C_3N is not sufficient to stabilize the diamane structure. The unsubstituted surface of NCCC must be reconstructed to be the Pandey π chain in order to stabilize the bonding between layers. On the other hand, CNCC cannot be stabilized in any cases because the electrons may not form the lone electron pair on the N-substituted side. Herein, π-C_3N and NCCN are shown that they can enhance the stabilization of diamondlike carbon film with nonpassivation where NCCN is energetically favorable at 10 GPa comparing with the layered phases of carbon nitride. They also keep the high values of elastic constants as comparable as diamond which potentially present superhard properties.

ACKNOWLEDGMENTS

This research project was supported by the Second Century Fund (C2F), Chulalongkorn University. It is partially supported by the Super SCI-IV Research Grant, Faculty of Science and Ratchadaphiseksomphot Endowment Fund of Chulalongkorn University, Grant for Research. Financial support was partially provided by Thailand Science Research and Innovation (TSRI) and the Synchrotron Light Research Institute (SLRI). A.E. acknowledges support from the Thailand Toray Science Foundation (TTSF). The Computational Materials Physics (CMP) Project, SLRI, Thailand, is acknowledged for providing a computational resource.

[1] Y. Gao, T. Cao, F. Cellini, C. Berger, W. A. de Heer, E. Tosatti, E. Riedo, and A. Bongiorno, Nat. Nanotechnol. **13**, 133 (2018).

[2] A. P. M. Barboza, M. H. D. Guimaraes, D. V. P. Massote, L. C. Campos, N. M. B. Neto, L. G. Cancado, R. G. Lacerda, H. Chacham, M. S. C. Mazzoni, and B. R. A. Neves, Adv. Mater. **23**, 3014 (2011).

[3] B. N. Davidson and W. E. Pickett, Phys. Rev. B **49**, 14770 (1994).

[4] K. C. Pandey, Phys. Rev. B **25**, 4338 (1982).

[5] A. Scholze, W. G. Schmidt, and F. Bechstedt, Phys. Rev. B **53**, 13725 (1996).

[6] S.-T. Lee and G. Apai, Phys. Rev. B **48**, 2684 (1993).

[7] A. Freedman and C. D. Stinespring, Appl. Phys. Lett. **57**, 1194 (1990).

[8] A. Freedman, J. Appl. Phys. **75**, 3112 (1993).

[9] L. A. Chernozatonskii, P. B. Sorokin, A. G. Kvashnin, and D. G. Kvashnin, JETP Lett. **90**, 134 (2009).

[10] A. G. Kvashnin and P. B. Sorokin, J. Phys. Chem. Lett. **5**, 541 (2014).

[11] A. G. Kvashnin, D. G. K. P. V. Avramov, L. A. Chernozatonskii, and P. B. Sorokin, J. Phys. Chem. C **121**, 28484 (2017).

[12] T. Pakornchote, A. Ektarawong, B. Alling, U. Pinsook, S. Tancharakorn, W. Busayaporn, and T. Bovornratanaraks, Carbon **146**, 468 (2019).

[13] L. G. P. Martins, M. J. S. Matos, A. R. Paschoal, P. T. C. Freire, N. F. Andrade, A. L. Aguiar, B. R. A. Neves, A. B. de Oliveira, M. S. C. Mazzoni, A. G. S. Filho, and L. G. Cançado, Nat. Commun. **8**, 96 (2017).

[14] F. Piazza, K. Gough, M. Monthioux, P. Puech, I. Gerber, R. Wiens, G. Paredes, and C. Ozoria, Carbon **145**, 10 (2019).

[15] P. V. Bakharev, M. Huang, M. Saxena, S. W. Lee, S. H. Joo, S. O. Park, J. Dong, D. C. Camacho-Mojica, S. Jin, Y. Kwon, M. Biswal, F. Ding, S. K. Kwak, Z. Lee, and R. S. Ruoff, Nat. Nanotechnol. **15**, 59 (2020).

[16] F. Piazza, M. Monthioux, P. Puech, and I. Gerber, Carbon **156**, 234 (2020).

[17] G. Kresse and J. Furthmüller, Comput. Mater. Sci. **6**, 15 (1996).

[18] G. Kresse and J. Furthmüller, Phys. Rev. B **54**, 11169 (1996).

[19] P. E. Blöchl, Phys. Rev. B **50**, 17953 (1994).

[20] P. E. Blöchl, O. Jepsen, and O. K. Andersen, Phys. Rev. B **49**, 16223 (1994).

[21] J. P. Perdew, K. Burke, and M. Ernzerhof, Phys. Rev. Lett. **77**, 3865 (1996).

[22] A. V. Krukau, O. A. Vydrov, A. F. Izmaylov, and G. E. Scuseria, J. Chem. Phys. **125**, 224106 (2006).

[23] H. J. Monkhorst and J. D. Pack, Phys. Rev. B **13**, 5188 (1976).

[24] J. D. Pack and H. J. Monkhorst, Phys. Rev. B **16**, 1748 (1977).

[25] S. Grimme, J. Antony, S. Ehrlich, and H. Krieg, J. Chem. Phys. **132**, 154104 (2010).

[26] A. Togo, F. Oba, and I. Tanaka, Phys. Rev. B **78**, 134106 (2008).

[27] A. Togo and I. Tanaka, Scr. Mater. **108**, 1 (2015).

[28] B. Pamuk and M. Calandra, Phys. Rev. B **99**, 155303 (2019).

[29] See Supplemental Material at http://link.aps.org/supplemental/10.1103/PhysRevB.102.075418 for the information on crystal structures, vibrational frequencies, and the method used to calculate the elastic constants of 2D materials in VASP.

[30] S. V. Bondarchuk and B. F. Minaev, New J. Chem. **41**, 13140 (2017).

[31] J.-Y. You, Z. Zhang, X.-J. Dong, B. Gu, and G. Su, Phys. Rev. Research **2**, 013002 (2020).

[32] C. Kittel, *Introduction to Solid State Physics*, 8th ed. (Wiley, Hoboken, NJ, 2005).

[33] D. M. Teter and R. J. Hemley, Science **271**, 53 (1996).

[34] X. Wei, B. Fragneaud, C. A. Marianetti, and J. W. Kysar, Phys. Rev. B **80**, 205407 (2009).

[35] Y. Ding and Y. Wang, J. Phys. Chem. C **117**, 18266 (2013).

[36] F. Mouhat and F.-X. Coudert, Phys. Rev. B **90**, 224104 (2014).

[37] H. J. McSkimin and P. Andreatch, J. Appl. Phys. **43**, 2944 (1972).

[38] A. Jain, S. P. Ong, G. Hautier, W. Chen, W. D. Richards, S. Dacek, S. Cholia, D. Gunter, D. Skinner, G. Ceder, and K. A. Persson, APL Mater. **1**, 011002 (2013).

[39] H. Dong, A. R. Oganov, Q. Zhu, and G. Qian, Sci. Rep. **5**, 9870 (2015).

[40] C. J. Pickard, A. Salamat, M. J. Bojdys, R. J. Needs, and P. F. McMillan, Phys. Rev. B **94**, 094104 (2016).

[41] C. J. Pickard and R. J. Needs, Phys. Rev. Lett. **102**, 125702 (2009).

[42] D. Smith, R. T. Howie, I. F. Crowe, C. L. Simionescu, C. Muryn, V. Vishnyakov, K. S. Novoselov, Y. Kim, M. P. Halsall, E. Greogoryanz, and J. E. Proctor, ACS Nano **9**, 8279 (2015).

[43] T. Pakornchote, Z. M. Geballe, U. Pinsook, T. Taychatanapat, W. Busayaporn, T. Bovornratanaraks, and A. F. Goncharov, Carbon **156**, 549 (2020).

[44] K. Okano, S. Koizumi, S. R. P. Silva, and G. A. J. Amaratunga, Nature (London) **381**, 140 (1996).

[45] S. Bhattacharyya, O. Auciello, J. Birrell, J. A. Carlisle, L. A. Curtiss, A. N. Goyette, D. M. Gruen, A. R. Krauss, J. Schlueter, A. Sumant, and P. Zapol, Appl. Phys. Lett. **79**, 1441 (2001).